Hindawi
Advances in Civil Engineering
Volume 2023, Article ID 2035247, 15 pages
https://doi.org/10.1155/2023/2035247

Research Article

Heat Transfer Enhancement of Energy Pile with Nanofluids as Heat Carrier

Ruizhi Wang,[1] Ya Yin,[2,3] Qingwen Li,[2,3] Xiao Hai,[4] Naifu Deng,[2] and Chao Huang[5]

[1]*School of Architecture, Tsinghua University, Beijing 100084, China*
[2]*Beijing Key Laboratory of Urban Underground Space Engineering, University of Science and Technology Beijing, Beijing 100083, China*
[3]*Jianlong Group & USTB Joint Laboratory, University of Science and Technology Beijing, Beijing 100083, China*
[4]*Benxi Longxin Mining Co., Ltd., Benxi 117000, China*
[5]*School of Computer & Communication Engineering, University of Science and Technology Beijing, Beijing 100083, China*

Correspondence should be addressed to Qingwen Li; qingwenli@ustb.edu.cn

Received 24 April 2023; Revised 20 July 2023; Accepted 10 September 2023; Published 29 September 2023

Academic Editor: Fujiao Tang

As one of the core components of the transport medium in the energy pile system, the circulating working fluid is crucial for the enhancement of its heat transfer efficiency. In this study, based on the heat transfer enhancement theory of nanofluids, deionized water was used as the base solution to prepare the corresponding 0, 0.5, 1, and 1.5 vol% nanofluids by introducing nanoparticles SiO_2, Al_2O_3, CuO, and Cu. The laws of thermal conductivity and specific heat capacity with the volume fraction of different nanofluids are studied by the comparison. The results of thermal conductivity research illustrate that the specific heat capacity of nanofluids decreases linearly with the increase of the volume concentration of nanoparticles, but the thermal conductivity increases linearly. The fluid with the highest thermal conductivity and specific heat capacity is Cu–water nanofluids. In addition, it is proposed to directly apply all kinds of nanofluids with 1 vol% as circulating fluid to self-made miniature model box of energy pile to simulate the working conditions in summer. The influence laws of the nanofluids on the flow rate and heat transfer efficiency in the energy pile were calculated through the temperature difference between the inlet and outlet of the heat exchange tube. The results reveal that the nanofluids used in the experiment exert a optimization influence on the heat transfer of energy pile but the mass flow rate of the nanofluids during the circulation is decreased compared with that of the deionized water circulation liquid. Among them, the temperature difference between inlet and outlet of Cu–water nanofluid is the largest, which has the best effect on improving the heat transfer efficiency of the energy pile but its mass flow loss is also the largest. The research results can provide a reliable reference for the improvement of heat transfer efficiency of energy pile engineering in the future.

1. Introduction

As a green and low-carbon renewable energy, geothermal energy will be the most important choice to replace the fossil energy. Geothermal energy can be divided into shallow, middle, and deep geothermal energy. The shallow geothermal energy is particularly suitable for the refrigeration and heating field of the buildings because of its low-mining cost and extremely convenient mining. The ground source heat pump is the most widely used shallow geothermal energy technology. The appearance of energy piles provides a new opinion for the extensive application of ground source heat pump, which has been widely used because of overcoming the shortcomings of traditional ground source heat pumps. At present, domestic and foreign scholars have carried out a large number of studies on energy piles, covering various aspects such as heat transfer mechanisms, heat exchange enhancement, thermal structural response, and group piles effects [1–7]. As one of the core components of the energy pile, the circulating working liquid carries heat and circulates in the heat exchanger under the working condition in summer, to release heat into the soil, and absorbs heat from the soil as it flows under the winter condition. Improving its heat transfer capacity will certainly improve the heat transfer

efficiency of energy pile, but there is a lack of research on this at present [8].

As an important medium for the heat transfer, the circulating working liquid's circulating efficiency and heat loss cannot be ignored for the overall heat exchange of the energy pile system. Therefore, it is exceedingly important to improve its heat transfer performance and heat exchange efficiency. One of the effective ways to improve the thermal conductivity of liquid is to apply metal, nonmetal, or oxide particles with high-thermal conductivity to the liquid. Combining solid particles with high-thermal conductivity with liquid into solid–liquid mixture is an effective way to improve the thermal conductivity of liquid. With the development of nanotechnology, it has attracted the attention of researchers due to its outstanding advantages such as low density, high conductivity, large specific surface area, and good optical properties [9, 10]. In the field of refrigeration and air conditioning, applying nanoparticles to refrigerants, lubricants, refrigerant carrier, and cryogen will have a broad prospect [11–15]. Therefore, many scholars have carried out a lot of research on applying nanofluids to the energy transport working medium to explore their enhanced heat transfer characteristics, energy consumption reduction, enhancement of coefficients of performance (COP), and energy efficiency [16–18].

These results indicate that nanoparticles can be introduced into the loop fluid to enhance the thermal properties of the fluid. Mixtures of nanoparticles in fluids have been extensively studied. In fluids with very low-particle concentration, the thermal performance of nanofluids will be significantly improved, which has been confirmed [19–21]. Das et al. [22] reviewed the properties of nanofluid heat transfer enhancement, nanofluid preparation methods, and theoretical models based on the fluid delamination, particle aggregation, and particle motion, revealing that the thermal conductivity of nanofluids increases with increasing temperature. Guerrieri et al. [23], Daneshipour and Rafee [24], and Lotfi et al. [25] have demonstrated that Al_2O_3–water, CuO–water, and multiwalled carbon nanofluid can enhance the heat transfer performance of the heat exchangers, respectively. And the total heat transfer coefficient of nanofluid is significantly improved by over water. Godson et al. [26], Ghozatloo et al. [27], and Bhanvase et al. [28] explored the heat transfer characteristics of silver/water nanofluids and graphene/water nanofluids with different concentrations in the heat exchanger, and found that the total heat transfer coefficient of nanofluids increased with the increase of particle concentration and Reynolds number. Khoshvaght-Aliabadi et al. [29] found that the flow rate of Cu–water nanofluid through the spiral microtubule was related to the curvature ratio, the weight concentration of the nanoparticles, the Prandt number and the Reynolds number. Sharma et al. [30] investigated the hydrodynamic characteristics of nanofluid flow through straight tubes and spiral coils. Ardekani et al. [31] represented that the dispersion and random motion of nanoparticles can improve the heat transfer properties of the fluid. Pathak et al. [32] proposed a magnetic fluid thin layer association with annular fin geometry to improve the shell-tube heat exchangers performance. A significant improvement has been observed in the system performance with more the 20% increase in efficiency of the AFMFG in both the fluid system. Wang et al. [33] studied that the thermal performance of an inclined miniature mesh heat pipe can be strengthened by using CuO nanofluid. Algarni et al. [34] studied the heat exchange performance of water nanofluids in a horizontal helical coil tube with constant temperature limitations. The result showed that the average heat transfer rises by 13% and 17% when nanoparticle volume fraction percentage density is 0.1%, 0.2%, and 0.3%. This paragraph describes a summary of research on the other nanofluids applied to enhance heat transfer performance in pipeline fluids, as well as Table 1.

Through the literature review, it is found that most existing studies focus on numerical or theoretical calculations, with few experimental studies, and there is almost no numerical model to verify data from the original experimental platform. In addition, the research on related nanofluids has not been applied to the energy pile systems, and their heat transfer effects and heat transfer impact laws during operation need to be revealed. Therefore, based on the analysis of nanofluid heat transfer enhancement theory, this study selects several common nanoparticles to prepare nanofluids, compares their thermal conductivity and specific heat capacity, and applies four types of nanofluids to the energy pile systems. The aim is to find out the nanofluid that is more suitable for the energy pile systems by comparing their overall heat transfer performance and economics, and to provide a reliable reference for the heat transfer theory system of the energy pile.

2. Theory of Heat Transfer Enhancement of Nanofluids

Nanofluids are particles of nanoscale size (1–100 nm) introduced to a liquid and suspended in it by certain means. Due to the small size of the nanoparticles, the particles exhibit a strong Brownian motion, which is beneficial for maintaining the stability of the suspension. Compared to ordinary fluids, nanofluids reflect enhanced heat transfer performance in the following aspects [43–45]:

(1) The addition of nanoparticles enhances the thermal conductivity of the original liquid (base fluid). The mechanism is broadly divided into two causes:

First, the thermal conductivity of nanoparticles is much higher than that of the liquid, and by adding nanoparticles, the basic structure of the original liquid is modified, resulting in enhanced internal heat transfer processes. The underlying principle is represented by the following equation:

$$k_{m,\mathrm{eff}} = \frac{k_p \phi \left(\frac{dT}{dx}\right)_p + k_f (1-\phi)\left(\frac{dT}{dx}\right)_f}{\phi \left(\frac{dT}{dx}\right)_p + (1-\phi)\left(\frac{dT}{dx}\right)_f}, \quad (1)$$

where $k_{m,\mathrm{eff}}$—the thermal conductivity of the nanofluid at rest (W/(m · K)); k_p—the thermal conductivity of the nanoparticles (W/(m · K)); k_f—the thermal conductivity of the original fluid (base fluid) (W/(m · K)); ϕ—volume ratio of the nanoparticles.

Table 1: Summary on application of nanofluid in conventional heat pipes.

Author	Types	Applications	Ratio	Research method	Main conclusions
Jiang [35]	Cu	Horizontal serpentine buried tube sandbox bench	1 and 3 wt%	Indoor tests and numerical simulations	(1) The stable maintenance time of 1 wt% Cu–water nanofluid with a mass ratio of 22 : 1 between nanocopper particles and sodium nitrite is the longest, but only 10 hr, which cannot meet the experimental requirements. The stability of suspension can be improved by increasing the concentration of dispersant in a certain range. The higher the concentration of Cu–water nanofluid, the shorter the stable suspension time (2) Cuo–water nanofluid improves the heat transfer performance of buried pipe, and the heat transfer ratio of horizontal snake buried pipe is close to 35% compared with water. Although the increase in the viscosity of the nanofluid leads to the increase of 16.4% in the running power of the pump, the use of Cuo–water nanofluid improves the heat transfer performance of horizontal snake buried pipe by close to 16% under the test condition
Diglio et al. [36]	Ag, Cu, Al, Al_2O_3, CuO, graphite, and SiO_2	Borehole heat exchanger	0.1, 0.2, 0.3, 0.4, 0.5, 0.6, 0.7, 0.8, 0.9, and 1 vol%	Numerical simulations	(1) Cu-based nanofluid is characterized by highest R_b reduction, that ranges from about 3.5%–3.8% varying ϕ from 0.1% to 1%, respectively; while, CuO-based nanofluid is the worst solution, with ΔR_b that varies from about 0.020%–0.20% (2) Ag-based nanofluid is characterized by highest convective heat transfer coefficient, following by Cu-based nanofluid (3) Cu- and CuO-based nanofluids are characterized by lowest volumetric heat capacity reduction, while graphite by highest one (4) Ag-based nanofluid is characterized by highest pressure drop, and it is followed by Cu-based nanofluid
Li et al. [37]	Al_2O_3, CuO, and SiO_2	*U*-shaped deep buried pipe	0.1, 0.3, 0.5, and 1–vol%	Indoor tests and numerical simulations	(1) CuO/water has the best effect on enhancing heat transfer in buried tubes, and the growth rate of the hourly average heat transfer per linear meter for 240 hr of buried tube heat transfer is calculated to be 0.624% at 1 vol% (2) The enhanced heat transfer effect of the same type of nanofluid increases with the increase of the volume concentration of nanoparticles, and the higher the volume concentration the more obvious the increase (3) The difference in the enhanced heat transfer effect of buried tubes is very small when the volume concentration of nanoparticles is the same for different types of nanofluids
Hassan and Harmand [38]	Cu, CuO, and Al_2O_3	Rotating heat pipes	0.04%	Numerical simulations	(1) Rotating heat pipes with Cu–water nanofluid have maximum heat transfer compared with CuO–water and Al_2O_3–water nanofluids. The maximum heat transfer by rotating heat pipe at $\Delta T = 20°C$ and $\omega = 3{,}000$ rpm increases by about 56% due to using Cu–water nanofluid with Cu nanoparticles of volume fraction 0.04 and radius 5 nm (2) The results show that for the same input conditions of the heat pipe and same volume fraction and diameter of solid nanoparticles, Cu–water nanofluid has the largest heat transfer compared with CuO–water and Al_2O_3–water nanofluids. Increasing taper angle of the condenser decreases the heat transfer of the rotating heat pipe for pure water and nanofluids
Niu et al. [39]	SiO_2	Miniature heat pipe	0%, 0.2%, 0.6%, and 1.0%	Indoor tests	(1) The utilization of SiO_2–water nanofluids as working fluids enhances the performance of the miniature heat pipe (2) As compared with the heat pipe using DI water, the decreasing of the thermal resistance in heat pipe using nanofluids is about 43.10%–74.46% by air cooling and 51.43%–72.22% by water cooling
Bhullar et al. [40]	Al_2O_3	Straight heat pipe	0.005, 0.05, 0.5, and 1.0 vol%	Indoor tests	(1) The experimental results show an optimum reduction of 22% in the thermal resistance value using 1 vol% of Al_2O_3/DI nanofluids as compared to DI water at low heat input of 12 W. The stabilized operation of the heat pipe is observed at high heat input of 73 W and at low concentration of 0.005 vol% Al_2O_3/DI water nanofluids

Table 1: Continued.

Author	Types	Applications	Ratio	Research method	Main conclusions
Barua et al. [41]	Al_2O_3 and MgO	The straight pipe and coiled pipe designs	0, 0.5, 1, 1.5, and 2 vol%	Indoor tests	(1) The nanofluids can significantly improve the heat and exergy gains. At the Reynolds number of 10, for the nanoparticles volume fraction of 2%, the heat gain of the nanofluid with MgO is about 6% greater than the nanofluid with Al_2O_3, and it is about 70% greater than the base fluid (water). The nanofluid with MgO nanoparticles shows better heat and exergy gains compared to the nanofluid with Al_2O_3 nanoparticles
Kumaresan et al. [42]	CuO	Sintered wick heat pipe	0.5, 1.0, and 1.5 wt%	Indoor tests	(1) The increase in heat transport capacity of the heat pipe is about 31.2% for 1 wt% of CuO nanofluid (2) Thermal resistance of heat pipe is also reduced when the DI water is replaced by CuO nanofluid and the changes observed for 0.5, 1.0 and 1.5 wt% are 38.3%, 66.1% and 54.1%, respectively (3) The thermal conductivity of heat pipe increases with the use of nanoparticles and its concentration. The enhancement registered for 0.5, 1.0 and 1.5 wt% are 46.6%, 63.5% and 55.9%, respectively. Thermal efficiency of heat pipe is improved by 24.9% for 1.0 wt% CuO nanofluid compared with the DI water at the optimum tilt angle of 45
Ghozatloo et al. [27]	Graphene	Shell and tube heat exchanger	0.05, 0.075 and 0.1 wt%	Indoor tests	(1) The effect of graphene on thermal conductivity of nanofluids is much more than heat transfer coefficient of nanofluids and this effect increases with increasing the concentration of graphene. The thermal conductivity of graphene nanofluids at 25 °C increased by 15.0%, 29.2 and 12.6 at 0.05, 0.075, and 0.1 wt%, respectively (2) With increasing graphene concentration and fluid temperature, the heat transfer coefficient of graphene nanofluids will be enhanced. By increasing the temperature from 25 to 38 °C, 13.1% increase in the convective heat transfer of 0.1 wt% graphene nanofluids was observed. The effect of graphene concentration in water at higher temperatures is more noticeable. By increasing the concentration of graphene from 0.025 to 0.1 wt%, the heat transfer coefficient of graphene nanofluids increased by 15.3% at 25°C, whereas at 38°C, an enhancement of 23.9% on heat transfer coefficient was occurred

Equation (1) shows that the internal heat transfer of the nanofluid is influenced by the thermal conductivity and volume ratio of the nanoparticles. The larger these two values are, the higher the thermal conductivity of nanofluid and the more rapidly its internal heat transfer. Second, nanoparticles move irregularly under the action of microscopic forces such as Brownian forces. Its micromotion contributes to the microconvection among the nanoparticles and the liquid, which enhances the heat transfer between the nanoparticles and the liquid molecules, and its macroscopic manifestation is the increase of the thermal conductivity of the liquid.

In summary, the additional value of the thermal conductivity due to microconvection of the nanofluid is set to k_b. According to Fourier's law of thermal conductivity, the equation for the thermal conductivity of a nanofluid can be given as follows:

$$-k_{nf}\nabla T = -k_{m,\text{eff}}\nabla T - k_b\nabla T, \tag{2}$$

where k_{nf}—the actual thermal conductivity of the nanofluid (W/(m · K)).

Equation (2) illustrates that the actual thermal conductivity of the final nanofluid is the sum of the thermal conductivity of the fluid structure change ($-k_{m,\text{eff}}$) and the additional value of the thermal conductivity of the microconvection formation (k_b).

(2) The addition of nanoparticles enhances the convective heat transfer coefficient of the fluid. The Brownian motion of nanoparticles enhances the interaction between the particles and the fluid molecules and the tube wall, reducing the thickness of the laminar sublayer and the thermal boundary layer. This leads to an increase in the temperature gradient in the inner laminar layer, i.e., the heat transfer efficiency between the surface of the tube wall and the nanofluid increases, which is macroscopically expressed as the enhancement of the convective heat transfer coefficient of liquid. The convective heat transfer coefficient of nanofluids involves a variety of factors and the relationship is complex. In general, the convective heat transfer coefficient of a nanofluid is expressed as a function of the following variables:

$$N_u = f\left(R_{e_{nf}}, P_{r_{nf}}, \frac{k_d}{k_f}, \frac{(\rho c_p)_d}{(\rho c_p)_f}, \phi, s\right), \tag{3}$$

where, $R_{e_{nf}}$—the Reynolds number of the nanofluid; $P_{r_{nf}}$—Planet number of the nanofluid; k_d—the thermal conductivity of the nanoparticle; $(\rho c_p)_d$—heat capacity of the nanoparticles; $(\rho c_p)_d$—the heat capa city of the original fluid; s—the shape and size of the nanoparticles.

The heat transfer mechanisms described by Equations (1) and (2) illustrate that the heat transfer performance of nanofluids is influenced by multiple factors, and the properties of the nanoparticles themselves play a significant role in the final performance of the nanofluids. Subsequently, the subsequent will select several common nanoparticles and prepare corresponding nanofluids to measure their thermophysical parameters. The nanofluids will be applied to energy piles to investigate the heat transfer performance of the nanofluids and their impact on the heat transfer efficiency of energy piles.

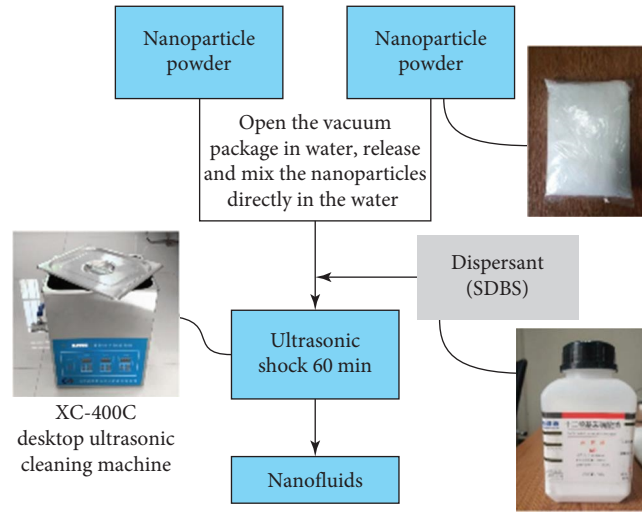

Figure 1: Nanofluid preparation process.

3. Preparation of Nanofluids

Nanofluids were synthesized by a "two-step method" using water as the base solution. The advantages of the two-step method are simple, economical, suitable for oxide nanoparticles, and large-scale production. The preparation process is shown in Figure 1. In order to increase the dispersion and stability of the nanoparticles in water, the dispersant was included [46]. Finally, in order to obtain a stable suspended nanofluid, the solid–liquid mixture was oscillated by ultrasonic to make the nanoparticles evenly distributed in the liquid.

Several common nanoparticles (SiO_2, Al_2O_3, CuO, and Cu) were selected for this experiment. The transmission electron microscopy (TEM) image of the nanoparticles is shown in Figure 2. Srihara et al. [47] pointed out that nanoparticles exhibit a higher surface area to volume ratio, which leads to higher heat transfer rates. The shapes of the four types of nanoparticles were all approximately spherical, so it was not possible to compare the heat transfer properties of the nanoparticles based on the surface area to volume ratios. Each group was prepared using a "two-step method" to prepare nanofluids with volume concentrations of 0.5%, 1%, and 1.5% using deionized water as the base liquid. Dispersants have important effects on the dispersion stability of nanofluids, and also on other properties of nanofluids (such as thermal conductivity, viscosity etc.) [48]. The optimal dispersant concentration can significantly improve the stabilit and thermal conductivity of the nanofluids [49]. Sodium dodecyl benzene sulfonate (SDBS) is a commonly used

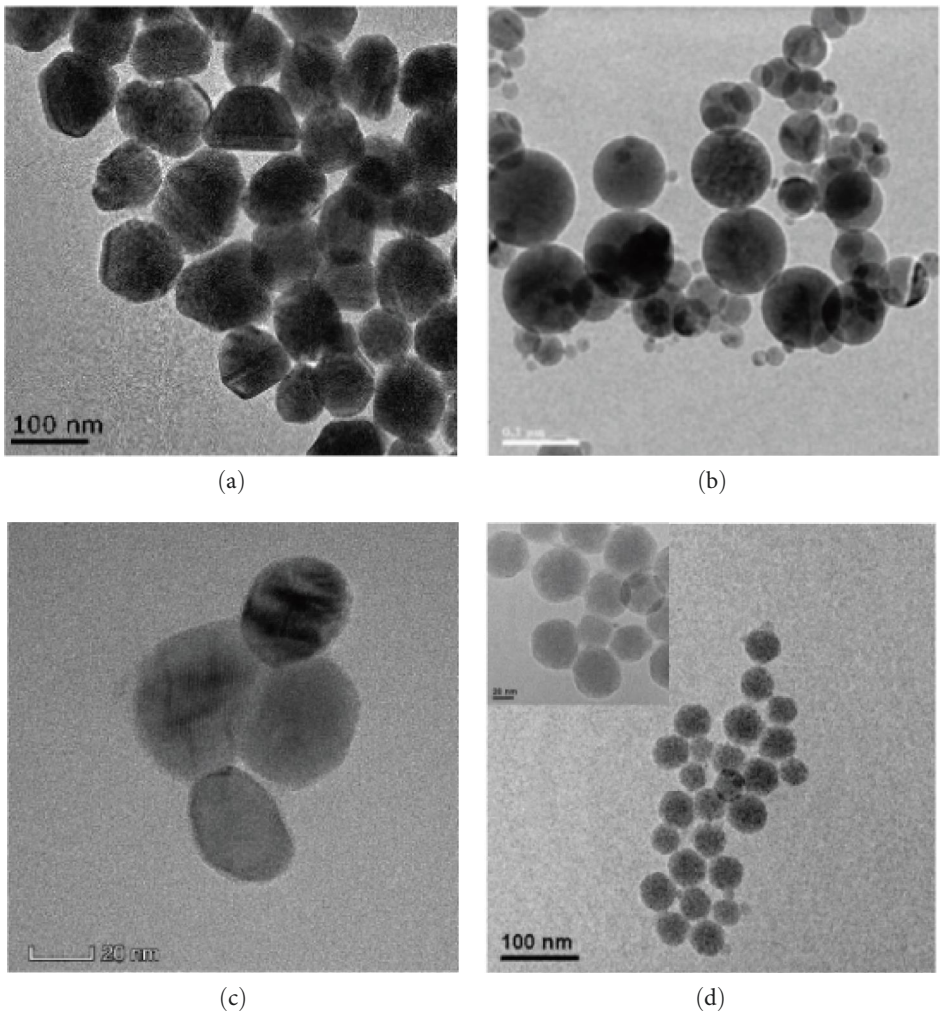

Figure 2: TEM photograph of nanoparticles (a) Cu, (b) Al_2O_3, (c) CuO, and (d) SiO_2 [35, 40, 50, 51].

anionic surfactant. SDBS is used as dispersing agents in the preparation of Cu–water, Al_2O_3–water, ZrO_2–water, and multiwalled carbon nanotubes nanofluids, as described in detail in Table 2. Moreover, SDBS is often used as dispersing agent for the industrial preparation of nanofluids. Therefore, 1 wt% SDBS was used as dispersant in this study.

SiO_2 nanopowder, average particle size 20 nm, purity 99.9%, spherical, and white.

Al_2O_3 nanopowder, average particle size 30 nm, purity 99.9%, α phase, and white.

CuO nanopowder, average particle size 30 nm, purity 99.9%, spherical, and black.

Cu nanopowder, average particle size 30 nm, purity 99.9%, spherical, and purplish red.

At the same time, in order to verify the role of dispersant and ultrasonic oscillation, and determine the preparation conditions of nanofluid, five nanofluid samples under the different conditions were prepared using nano-Al_2O_3 powder. Deionized water and nanoparticles were mixed under the following different conditions: (1) neither dispersant nor ultrasonic oscillation was included; (2) only dispersant was included without ultrasonic oscillation; (3) apply dispersant and shake for 30 min; (4) apply dispersant and shake for 60 min; (5) apply dispersant and shake for 90 min. The dispersion stability of the nanofluid was preliminarily evaluated using the settling method. The dispersion stability of the nanofluid was preliminarily assessed using the settling method. The prepared nanofluid was left for 10 days to settle under the ambient temperature and atmospheric pressure conditions. The results are shown in Figure 3.

As can be seen from the figure, the particles of sample (1) have been completely precipitated out of the water due to the absence of dispersant and ultrasonic oscillation. Due to the effect of dispersant, only a small amount of nanoparticles in sample (2) were suspended in water, and most of them had been precipitated. Samples (3), (4), and (5) have good dispersion and stability due to the addition of dispersant and ultrasonic oscillation at the same time. In particular, samples (4) and (5) have the best stability and meet the test requirements. Therefore, the preparation conditions of the nanofluid in the experiment were: adding 1 wt% of dispersant, subjecting it to ultrasonic oscillation for 60 min, and letting it stand for 10 days under the ambient temperature and atmospheric pressure conditions.

Table 2: Experimental results of the effect of surfactant on the stability of nanofluids [52].

Nanofluids	Particle concentration	Surfactant	Experimental results
$CuO–H_2O$	–	PAAS	0.4–0.8 wt%
$CuO–H_2O$	0.97 wt%	SDBS	1.94 wt%
$CuO–H_2O$	2, 4 wt%	SDBS	2, 4 wt%
$Cu–H_2O$	0.l wt%	SDBS, CTAB, OP	SDBS: 0.1 wt%
$Cu–H_2O$	0.l wt%	SDBS, CTAB, TX-10	SDBS: 0.07 wt%
$Al_2O_3–NH_3•H_2O$	0.l wt%	SDBS	0.l wt%
$Al_2O_3–H_2O$	0.l wt%	SDBS	0.l wt%
α-$Al_2O_3–H_2O$	—	SHP, CTAC, PEG400, SDBS	SDBS: 2.0 wt%
γ-$Al_2O_3–H_2O$	2.0 wt%	PEG600, T-80, SDBS, SDS	PEG600: 0.1 wt%
$TiO_2–H_2O$	0.l wt%	SDS	0.l wt%
$TiO_2–H_2O$	0.7 wt%	SDBS, CTAB, PVP	SDBS: 0.21 wt%
$TiO_2–H_2O$	20 mg/L	SDBS, CTAC, Span80	SDBS: 25 mg/L
$SiO_2–H_2O$	2.5 wt%	TTAB, CTAB, OTAB	CTAB: 1.4 mmol/L
$MWNT–H_2O$	—	SDBS, HTAB, OP	OP: 1.5 mL/L
$MWNT–H_2O$	0.5 wt%	12-3-12, $2Br^{-1}$	0.6 wt%

Figure 3: Results of nanofluid standing for 10 days.

4. Study of the Thermal Conductivity of Nanofluids

The thermal conductivity was tested using the KD2pro portable thermal conductivity meter produced by DECAGON in the United States, which uses a KS-1 needle probe. The heat capacity was tested using a differential scanning calorimeter (DSC) in the United States. The testing instruments are shown in Figure 4.

The DSC method uses a sapphire of known heat capacity as the reference material and an aluminum pot as the measuring container. The DSC curve was measured three times: the first time was the heat flow curve of the empty crucible, which served as the baseline; the second time was the curve of the sapphire when it was heated, which served as the standard line; and the third time was the heat flow curve of the sample being measured. Based on these three heat flow curves, the heat capacity of the sample was calculated using Equation (4):

$$c_{p,\text{sample}} = \frac{Q_{\text{sample}} - Q_{\text{blank}}}{Q_{\text{sapphire}} - Q_{\text{blank}}} \cdot \frac{m_{\text{sapphire}}}{m_{\text{sample}}} \cdot c_{p,\text{sapphire}}. \quad (4)$$

In Equation (4), $c_{p,\text{sample}}$ and $c_{p,\text{sapphire}}$ are the heat capacities of the sample and sapphire, respectively; Q_{sample}, Q_{blank}, and Q_{sapphire} are the heat flows of the sample being measured, the empty crucible, and the sapphire; m_{sapphire} and m_{sample} are the masses of the sapphire and sample, respectively.

When measuring the thermal conductivity coefficient, choose the KS-1 probe, connect it to the KD2pro host, and insert the probe into a test tube containing the nanofluid. After insertion, the probe was first left to stand for 10 min to allow the temperature of the probe and nanofluid to equilibrate while preventing the liquid disturbance caused by the probe insertion from affecting the accuracy of the measurements. Measurements were then carried out using the KD2pro host. The KD2pro conducted a small heating operation on the liquid through the probe. The measurement cycle included equilibrium, heating, and cooling, and the temperature change of the liquid during this period was measured. Then the nonlinear least squares program was used to fit the measured results by an exponential integral function to determine the thermal parameters of the liquid. During this measurement process, it is important to keep the environmental conditions as stable as possible to prevent the environmental disturbances from affecting the accuracy of the measurement results.

4.1. Specific Heat Capacity of Nanofluids. The experiment used DSC to measure the specific heat of four different volume concentrations of nanofluids and converted them into specific heat capacity as shown in Figure 5 and the following conclusions can be drawn:

(1) From the data in Figure 5, the specific heat capacities of the fluids after the nanoparticle addition all decreased to varying degrees. Among them, Cu–water and CuO–water nanofluids decreased the least, with a specific heat capacity of about 4.12 and 4.10 J/(g · K) at 1.5 vol%, a decrease of 1.7% and 2.1%, respectively. Second, the specific heat capacity of the Al_2O_3–water

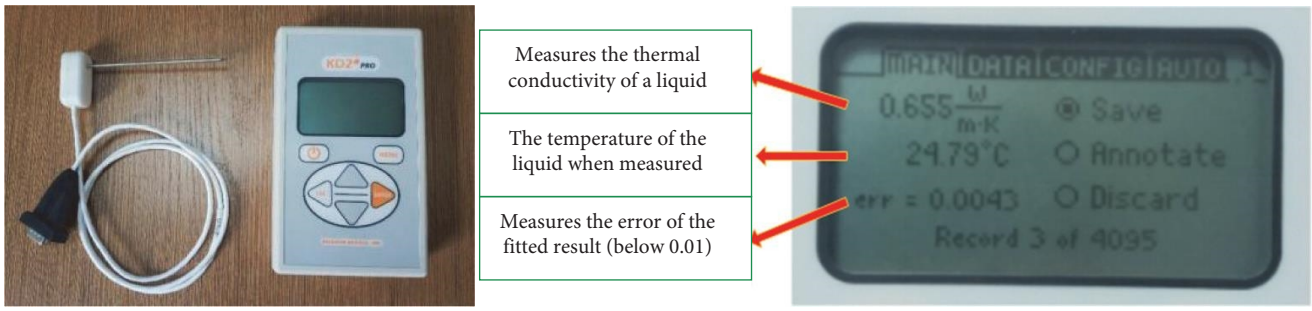

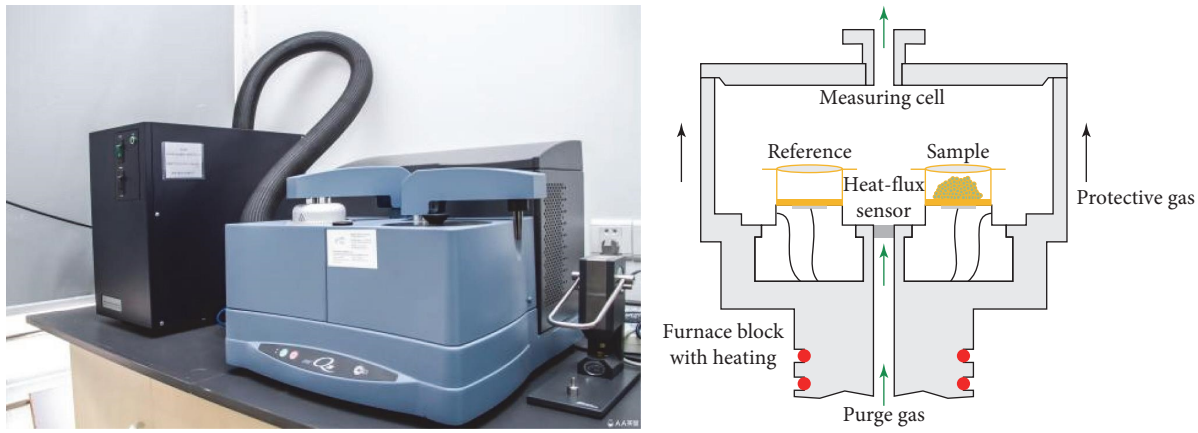

Figure 4: Thermal properties testers (KD2pro and DSC).

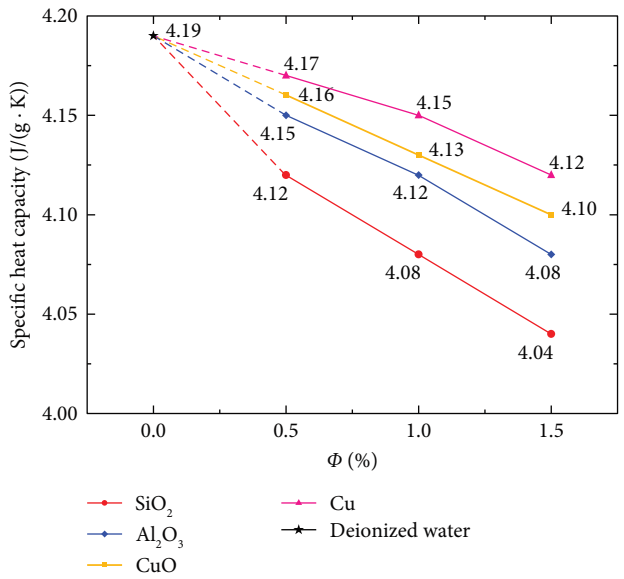

Figure 5: Measured specific heat capacity of different nanofluids.

nanofluid decreased relatively less, with a specific heat capacity of about 4.08 J/(g · K), a decrease of 2.6%. SiO_2–water nanofluid decreased the most, giving a specific heat capacity of around 4.04 J/(g · K), a decrease of 3.6% at 1.5 vol%.

(2) The tendency in Figure 5 represents that the specific heat capacity of the nanofluid decreases essentially linearly with the addition of nanoparticles. This indicated that the amount of heat carried by the fluid per unit mass had decreased, which may be detrimental to the heat transfer performance of the pipeline.

4.2. Thermal Conductivity of Nanofluids. The experiments were carried out using KD2pro to measure the thermal conductivity of four groups of nanofluids at different volume concentrations. Figure 6 was drawn, and the following conclusions could be obtained:

(1) From the data in Figure 6, it can be seen that the thermal conductivity of the fluid after the addition of nanoparticles was all greater than that of pure water. Among them, Cu–water nanofluid had the highest thermal conductivity enhancement, with its thermal conductivity (at 25°C) reaching 0.701 W/(m · K) at 1.5 vol%, an increase of 15% compared to pure water. The thermal conductivity enhancement of Al_2O_3–water and CuO–water nanofluids was similar, with a thermal conductivity of 0.655 W/(m · K) at a volume fraction of 1.5%, an increase of 7.6% compared to pure water. SiO_2–water nanofluid showed the worst improvement in thermal conductivity, with a thermal conductivity of 0.637 W/(m · K), an increase of only 4.5% compared to pure water.

(2) The trend in Figure 6 shows that the increase in thermal conductivity of the nanofluid increases essentially linearly with the volume fraction of nanoparticles. This indicated that increasing the amount of nanoparticles applied to water within a certain range can continuously enhance the thermal conductivity of the nanofluid. However, high-thermal conductivity

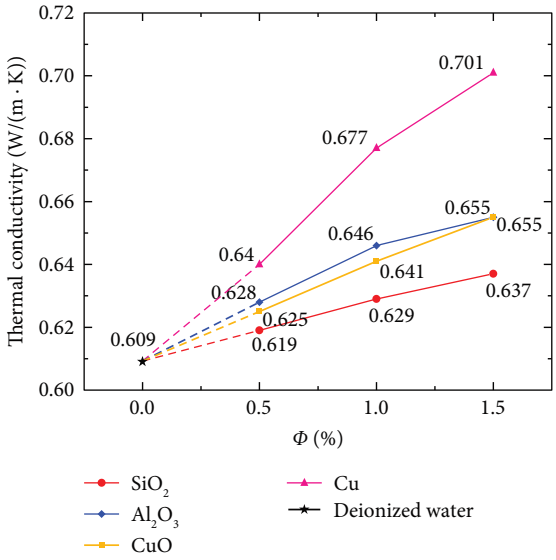

Figure 6: Measured thermal conductivity of different nanofluids.

did not necessarily mean high-thermal performance, and Figure 5 shows that the addition of nanoparticles also reduces the specific heat capacity of the nanofluid itself.

In fact, the addition of nanoparticles had a more pronounced improvement in the convective heat transfer coefficient of nanofluids, which played a crucial role in the pipeline heat transfer. In the case of CuO–water nanofluids, for example, Li et al. [53, 54] demonstrated that under laminar flow conditions (Re = 1200), the convective heat transfer coefficient was improved by about 25% compared to pure water, and under the some turbulent flow conditions the improvement was even greater, up to 60%. The effect of nanofluid on the convective heat transfer coefficient was generally 1.5–4 times that of the thermal conductivity coefficient. The application of nanofluids to energy piles may improve the heat transfer efficiency of energy piles. In fact, Equation (3) illustrated that the convective heat transfer coefficient was affected by many factors, and its value varies greatly. Measuring the convective heat transfer coefficient of nanofluid alone had little effect on predicting the heat transfer effect of the energy pile. Therefore, the nanofluid will be directly applied to the energy pile, so as to visually observe the influence of nanofluid on the heat transfer efficiency of energy pile.

5. Nanofluids on Energy Pile

Based on the heat storage method, the formula for evaluating the summer heat exchange capacity of the energy pile is

$$q = \frac{Q}{\tau} = \frac{\int_0^{\tau} m_f C_{p_f} \Delta T_f d\tau}{\tau}, \quad (5)$$

where q—the heat exchange efficiency of energy pile (W); Q—the cumulative heat exchange of energy pile (J); c_{pf}—the specific heat capacity of the fluid (J/(kg · K)); m_f—mass flow rate of the fluid in the heat exchanger pipe (kg/s); ΔT_f—the temperature difference of the heat carrier medium at the inlet and outlet (°C); τ—the exchange time (s).

It can be seen from Figures 5 and 6 that with the addition of nanoparticles, the thermal conductivity of nanofluids has been greatly improved compared with that of pure water. However, its specific heat capacity is reduced, and the addition of nanoparticles also changes the performance of the liquid. Therefore, the effect m_f on the Equation (5) is not known, and thus the effect on the heat transfer capacity of the energy pile cannot be judged at this point. In this section, the effect of nanofluid will be verified by simulating the summer conditions of the energy pile using a model box.

5.1. Introduction to the Energy Pile Model Box. A box-type similiar model of energy pile is basically a cube with a side length of 2 m. The main body is made of steel plates and bars welded together, and one side of which is explosion-proof glass, from the outside the filling of the soil in the box can be observed, as in Figure 7. The experiments can be carried out by placing prefabricated energy piles inside the box and compacting the fill, which consists of:

(1) Energy pile

Translation:

The energy pile was 1.6 m long and 0.1 m in diameter, made of ordinary concrete according to the concrete mix ratio in the "Code for Design of Concrete Structures" (JGJ-55-2011) [55]. The steel bar inside the pile was model HRB335 with a diameter of 10 mm. The inner diameter of the buried pipe inside the pile was 5 mm and the outer diameter was 7 mm. The form of the buried pipe was spiral, with a pitch of 80 mm, a diameter of 0.08 m. The inlet of the buried pipe was located at the top of the pile. After the fluid enters from the inlet, it flows along the spiral tube to the bottom, and then rises from the straight tube to the top of the pile.

(2) Soil

The soil was made from the local chalky clay and its parameters were measured as follows: density of 1.92 g/cm^3, moisture content of 10.3%, and specific gravity of 2.7. The soil was filled layer by layer from the bottom of the box upwards. And every time a certain amount of soil was added to the box, the filling was stopped and compacted using a geotechnical hammer. The soil near the energy pile was hitting repeatedly to ensure the full contact between the energy pile and the soil, and the accuracy of the results was guaranteed. During the gradual filling of the soil, the sensors were installed at depth and full contact with the soil was ensured. There were four piles in the model box, and only one pile was set up with a heat transmitter on the inside of the pile, allowing the temperature change of the soil around that pile to be measured. The overall arrangement is shown in Figure 6.

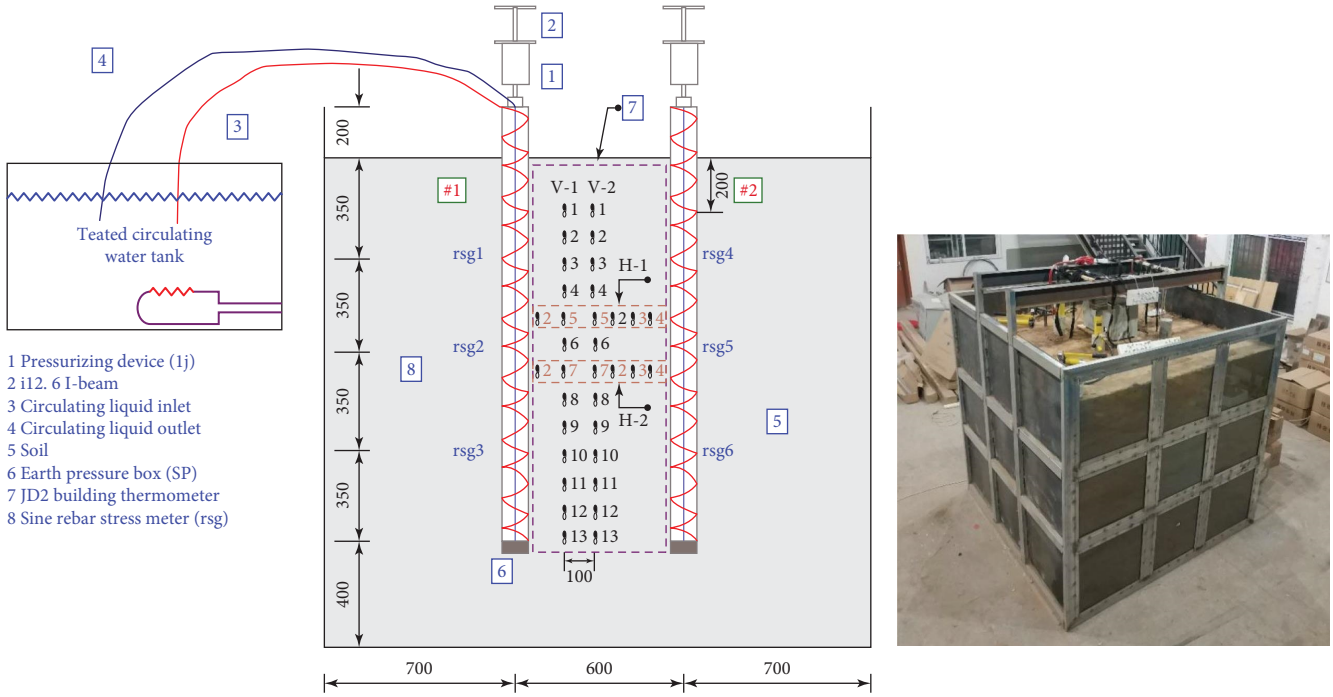

Figure 7: Model box design drawing and physical drawing.

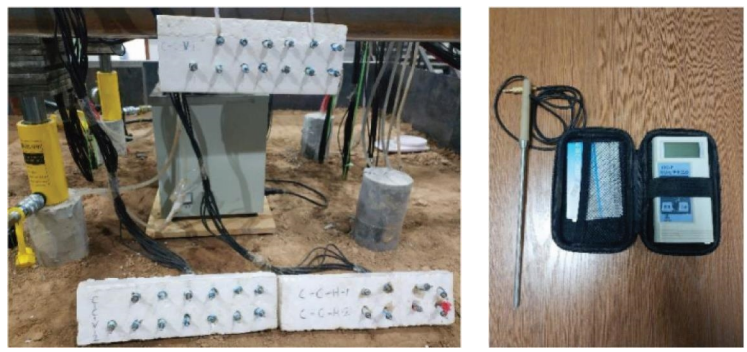

(a) (b)

Figure 8: Model box temperature measurement system: (a) temperature measurement panel and (b) JDC-2 electronic building pyrometer.

(3) Working fluid circulation system

In order to simulate the fluid temperature at the inlet to the energy pile, HH-420 constant temperature circulating water tank was used in the model box to ensure that the water temperature at the inlet was basically constant in the experiment. The circulating fluid was controlled by a submersible pump with a power of 10 W, which was connected to the inlet pipe at the top of the pile and placed into the thermostatic tank to drive the flow of fluid in the buried pipe.

(4) Test systems

The probe is embedded in the soil and the wire was extended to the surface to create a simple "temperature panel" with a JD2-2 electronic building thermometer, as shown in Figure 8. The model tank was located in the plant, where the temperature was relatively constant for the experiments.

5.2. Effect of Nanofluid on Flow in the Tube. In this energy pile heat exchange experiment, a nanofluid with different material volume fractions of 1% was used as the working fluid, and pure water was used as the control group. Moreover, the addition of nanoparticles changed the basic structure of the fluid, its viscosity, and resistance of the tube. Hence, it is deemed necessary to investigate the flow alterations of nanofluids in the energy pile prior to the official commencement of the experiment. The prepared fluid was placed into the tank, and the buried tube inlet was connected to the pump and the pump was switched on, keeping the power of the pump constant. The outlet of the buried tube

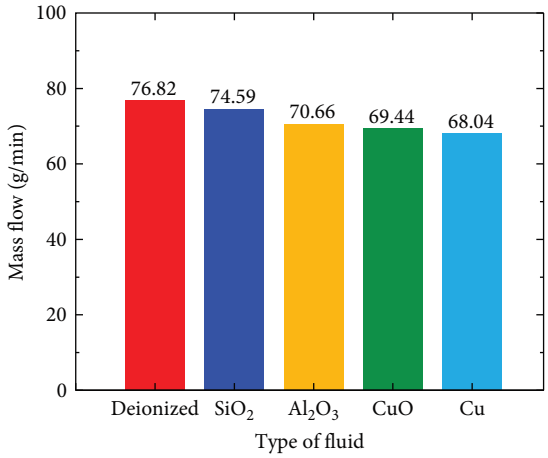

Figure 9: Measured mass flow rates for different fluids.

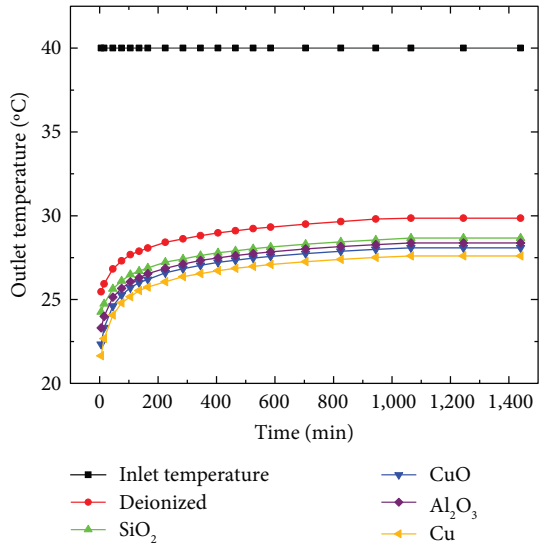

Figure 10: Measured fluid temperature at the outlet for different fluids.

was observed. And after a continuous uninterrupted flow of water appeared at the outlet, a beaker was used to take up the flow and the mass of fluid flowing out of the outlet was measured over a 10 min period. The mass data were converted to mass flow rate and plotted in Figure 9.

As can be seen from Figure 9, the nanofluids have different degrees of mass flow rate reduction compared to pure ionized water. The mass flow loss of SiO_2–water nanofluid was the least, with a decrease of 2.23 g/min compared to pure water, a decrease of 2.90%. The mass flow rate of Al_2O_3–water nanofluid decreased by 6.16 g/min, a decrease of 8.02%. The mass flow rate of CuO–water nanofluid was reduced by 7.38 g/min (9.61%). The mass flow loss of Cu–water nanofluid was the largest, which was reduced by 8.78 g/min (11.4%). This indicated that under the same pump power, the addition of nanoparticles made the resistance of the fluid rise, so the mass flow rate of the nanofluid had different degrees of loss, which was related to the type of nanoparticles added.

5.3. Experiments on the Heat Transfer Effect of Nanofluids. After the flow test, the nanofluid heat transfer experiment can be carried out. The experiment simulates the operation of the energy pile in summer, with the inlet water temperature set at 40 °C and the power of the pump set at 10 W, and ensuring that the inlet water temperature and pump power remain constant throughout the experiment.

Before the experiment initiated, the temperature sensor reading around the pile was read to record the initial soil temperature. The prepared nanofluid was succeeding poured into the thermostatic circulation tank, and the tank heater was activated. After the thermostatic tank had heated the fluid to 40°C and the temperature remained stable, the pump was started and the water temperature at the outlet was measured at regular intervals. In order to ensure the accuracy of measuring the water temperature, when measuring the outlet water temperature, the test directly sets the probe into the outlet pipe to measure the outlet water temperature at the first time, which was to prevent the result deviation caused by the conduction and convection of the liquid with the container, air etc. after flowing out. The running time for each nanofluid was set at 1,440 min and the soil temperature change was checked every 1–2 days. After the soil returned to the initial temperature, the heat transfer experiment of the next group of nanofluids was carried out to ensure the accuracy of the results. The data of the outlet water temperature for each nanofluid were recorded and plotted as the outlet water temperature curve with different fluids over time, as shown in Figure 10.

Combined with Figure 10, the following conclusions can be drawn:

(1) As the energy pile continued to work, the outlet water temperature under the different nanofluid conditions all gradually rose over time and stabilized, but there was still a gap from the inlet water temperature, which proved that the energy pile was operating normally and that the different fluids were exchanging heat with the surrounding medium.

(2) The outlet water temperature of pure water after stabilization was 29.8°C, a difference of 10.2°C from the inlet water temperature. Among the four nanofluids, the Cu–water nanofluid had the largest temperature change, with a difference of 12.4°C from the inlet water temperature, which was 22% higher than pure water. The second is Al_2O_3–water nanofluid, with a difference of 11.9°C from the inlet water temperature and 17% higher than pure water. After achieving stability, the temperature rise of CuO–water nanofluid was 11.7°C, which was 15% higher than that of pure water. The temperature change of SiO_2–water nanofluid was the smallest, rising 11.3°C, 11% higher than that of pure water.

Based on the specific heat capacity, mass flow and other data of the different fluids measured in previous sections, combined with Equation (5), the heat transfer efficiency of the energy pile with the application of different fluids can be calculated and plotted in Figure 11.

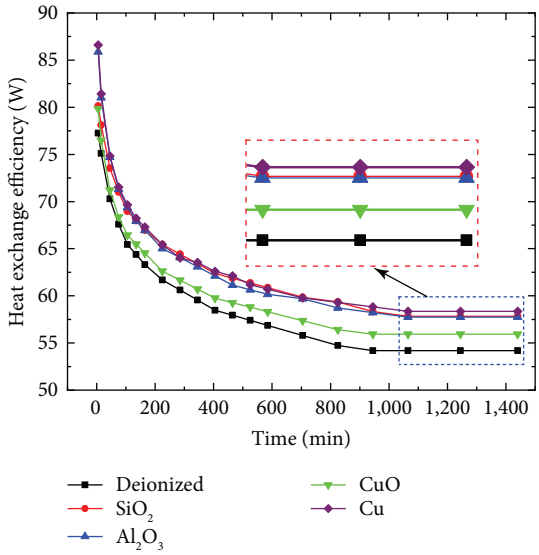

Figure 11: Calculated heat transfer efficiency for different fluids over time.

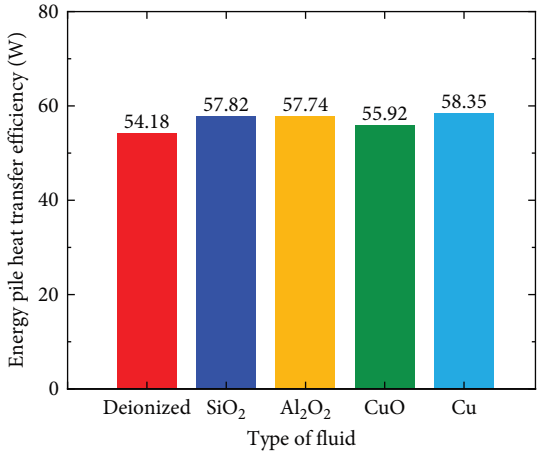

Figure 12: Calculated heat transfer efficiency of energy piles using different fluids.

By extracting the heat transfer efficiency data after reaching stability in the graph, Figure 12 is plotted. Combining Figures 11 and 12, the following conclusions can be drawn.

(1) Over time, the heat transfer efficiency of the energy piles with different fluids increases to varying degrees and eventually converges to a stable value.

(2) The heat transfer efficiency of the energy pile with pure water as the working fluid was 54.05 W after stabilization. Among the four nanofluids, the Cu–water nanofluid improved the heat transfer efficiency of the energy pile the most, with a stabilized heat transfer efficiency of 58.35 W, an increase of 7.70%. SiO_2–water nanofluid and Al_2O_3–water nanofluid have similar improvement effects on the heat transfer efficiency of the energy piles, with an increase of more than 6.72% and 6.57%. Although there was a significant difference between the water temperature at the inlet and outlet of the two, the mass flow loss of SiO_2–water nanofluid was more than insignificant. So the heat transfer efficiency of the two was similar in the end. Cuo–water nanofluid had little effect on improving the heat transfer efficiency of energy pile, and its heat transfer efficiency after stabilization was 55.92 W, with an increase of less than 3.21%. The main reason was that the energy pile using CuO–water nanofluid as the working fluid has severe flow losses, which limits the heat transfer improvement. The magnitude of the relationship among the data also suggested that the better the thermal conductivity of the nanofluid used, the lower the specific heat capacity and flow loss, the better the increase in the heat transfer efficiency of the energy pile.

6. Discussion and Conclusion

To verify the accuracy and reliability of the similar simulation study, the experimental findings were compared with the numerical results of the previous literature. The trend of the change in the specific heat capacity and thermal conductivity of the nanofluid tested in the experiment with the concentration of nanoparticles is consistent with existing research, and the data results have an error range of 0.24%–3.46% [37, 56]. Zhang [57] used numerical simulation to study the influence of different types of water-based nanofluids as working fluids on the heat transfer characteristics of ground source heat pump systems. The results found that the ground source heat pump system using water-based Cu nanofluid had better heat transfer characteristics, followed by SiO_2, Al, Al_2O_3, Fe_3O_4, and CuO nanofluids. This is consistent with the results of this study, and validates the results of the similar simulation study. In addition, Jiang [35] constructed a sandbox experimental platform for ground source heat pump systems and found through indoor similarity experiments that Cu–water nanofluid had the best heat transfer effect in horizontal serpentines, while Al–water nanofluid and SiO_2–water nanofluid had relatively poor heat transfer effects. The heat transfer performance was improved by 16% using CuO–water nanofluid under the experimental conditions. Diglio et al. [36] studied the influence of low-concentration (0.1–1 vol%) nanofluids (Cu, CuO, Ag etc.) on the thermal resistance of the vertical ground source heat pump system borehole through numerical calculations. The conclusion indicates that 1 vol% copper nanofluid has the best effect, which cost is about 12% of the total cost of ground source heat pump system. Leong et al. [58] simulated a shell-and-tube heat exchanger experiment, and the results showed that adding 1% Cu nanoparticles to ethylene glycol-based fluid increased the heat transfer rate by approximately 8.116%. This is similar to the efficiency increase of 7.70% in heat transfer of the Cu-nanofluid in this study. In summary, the research findings of this paper are reliable and can provide a reference for the application of nanofluids as circulation media in energy pile heat exchange pipes.

In this paper, according to the heat transfer enhancement mechanism of the energy pile, an attempt was made to promote the heat transfer performance of the circulating working fluid by using nanofluids of different types (SiO_2, Al_2O_3, CuO, and Cu) with different volume concentrations (0, 0.5, 1, and 1.5 vol%) instead of water as the working fluid of the energy pile. And by measuring the thermal parameters of the nanofluids and conducting summer working condition experiments of the energy pile model simulation, it was concluded that Cu–water nanofluid has the lowest outlet temperature and the best effect on the heat transfer efficiency of the energy pile. The specific results are as follows:

(1) The specific heat capacity of the nanofluid basically decreases linearly with the addition of nanoparticles. Among them, CuO and Cu–water nanofluids decreased the least, with a specific heat capacity of about 4.12 and 4.10 J/(g · K) at 1.5 vol%, followed by Al_2O_3–water nanofluids (4.08 J/(g · K)), and the specific heat capacity of SiO_2–water nanofluids decreased the most (4.04 J/(g · K)).

(2) The thermal conductivity of the nanofluids basically increases with the linearity of the volume fraction of nanoparticles. Among them, Cu–water nanofluids showed the highest enhancement in thermal conductivity (0.701 W/(m · K)), with a 15% increase compared to pure water at 1.5 vol%, followed by Al_2O_3, CuO, and SiO_2–water nanofluids (0.655, 0.655, and 0.637 W/(m · K)).

(3) Measurements of the mass flow rate of the nanofluids circulating within the energy pile revealed that the nanofluids all had varying degrees of mass flow rate loss relative to pure water, with SiO_2–water nanofluids losing the least mass flow rate, with a decrease of 2.23 g/min compared to pure water, followed by Al_2O_3 and CuO–water nanofluids. And Cu–water nanofluids losing the most mass flow rate, which is reduced by 8.78 g/min (11.4%). This indicates that the mass flow rate of the nanofluid is related to the type of nanoparticles applied.

(4) Over time, the heat transfer efficiency of the four nanofluids with 1 vol% as the circulating fluid of the energy pile decreased to different degrees during the working time and finally tended to a stable value. Among the four nanofluids, the Cu–water nanofluid had the greatest effect on the heat transfer efficiency of the energy pile, with an increase of 7.70%. The SiO_2 and Al_2O_3–water nanofluids has a similar effect on the heat transfer efficiency of the energy pile, and the CuO–water nanofluid has a minimal effect on the heat transfer efficiency, primarily due to its serious flow loss. This indicates that the better the thermal conductivity of the nanofluid used, the lower the specific heat capacity and flow loss, the better the improvement of the heat transfer efficiency of the energy pile.

Data Availability

The data used to support the findings of this study are included within the article.

Conflicts of Interest

The authors declare that they have no conflicts of interest.

Acknowledgments

This research was financially supported by the National Natural Science Foundation of China (52274107), Interdisciplinary Research Project for Young Teachers of USTB (FRF-IDRY-GD21-001), and Foshan Science and Technology Innovation Special Fund Funding Project (BK21BE014).

References

[1] Y. Yin, Q. Li, and L. Qiao, "Response of energy pile-soil structure and pile group effect: an indoor similarity simulation study," *Journal of Building Engineering*, vol. 51, Article ID 104247, 2022.

[2] Q. Li, Y. Yin, L. Kong, and L. Qiao, "Enhancing heat transfer in the heat exchange medium of energy piles," *Journal of Building Engineering*, vol. 40, Article ID 102375, 2021.

[3] L.-P. Kong, L. Qiao, Y.-Y. Xiao, and Q.-W. Li, "A study on heat transfer characteristics and pile group influence of enhanced heat transfer energy piles," *Journal of Building Engineering*, vol. 24, Article ID 100768, 2019.

[4] D. Wu, H. Liu, G. Kong, and C. Li, "Thermo-mechanical behavior of energy pile under different climatic conditions," *Acta Geotechnica*, vol. 14, no. 5, pp. 1495–1508, 2019.

[5] T. You and H. Yang, "Influences of different factors on the three-dimensional heat transfer of spiral-coil energy pile group with seepage," *International Journal of Low-Carbon Technologies*, vol. 15, no. 3, pp. 458–470, 2020.

[6] J. Fang, G. Kong, Y. Meng, L. Wang, and Q. Yang, "Thermomechanical behavior of energy piles and interactions within energy pile-raft foundations," *Journal of Geotechnical and Geoenvironmental Engineering*, vol. 146, no. 9, Article ID 04020079, 2020.

[7] Z. Chen, B. Wang, L. Zheng, H. Xiao, and J. Wang, "Research on heat exchange law and structural design optimization of deep buried pipe energy piles," *Energies*, vol. 14, no. 20, Article ID 6449, 2021.

[8] Q. Jiang, Y. Jiao, J. Luo, and H. Wang, "Review and prospect on heat transfer and bearing performance of energy piles," *Rock and Soil Mechanics*, vol. 40, no. 9, pp. 3351–3362 3372, 2019.

[9] J. Li, T. Wei, and J. Yan, "Preparation of graphene nanosheet/CoS_2 composite and its application in supercapacitors," *CIESC Journal*, vol. 65, no. 7, pp. 2849–2854, 2014.

[10] F. Li, "Investigation on photothermal conversion characteristics of graphene nanosheets-glycol nanofluids," *CIESC Journal*, vol. 71, no. S1, pp. 479–485, 2020.

[11] V. Nair, P. R. Tailor, and A. D. Parekh, "Nanorefrigerants: a comprehensive review on its past, present and future," *International Journal of Refrigeration*, vol. 67, pp. 290–307, 2016.

[12] A. A. M. Redhwan, W. H. Azmi, M. Z. Sharif, and R. Mamat, "Development of nanorefrigerants for various types of refrigerant based: a comprehensive review on performance,"

International Communications in Heat and Mass Transfer, vol. 76, pp. 285–293, 2016.

[13] W. H. Azmi, M. Z. Sharif, T. M. Yusof, R. Mamat, and A. A. M. Redhwan, "Potential of nanorefrigerant and nanolubricant on energy saving in refrigeration system: a review," *Renewable and Sustainable Energy Reviews*, vol. 69, pp. 415–428, 2017.

[14] A. Bhattad, J. Sarkar, and P. Ghosh, "Improving the performance of refrigeration systems by using nanofluids: a comprehensive review," *Renewable and Sustainable Energy Reviews*, vol. 82, pp. 3656–3669, 2018.

[15] N. A. C. Sidik, T. H. Kean, H. K. Chow, A. Rajaandra, S. Rahman, and J. Kaur, "Performance enhancement of cold thermal energy storage system using nanofluid phase change materials: a review," *International Communications in Heat and Mass Transfer*, vol. 94, pp. 85–95, 2018.

[16] G. Xie, H. Qi, G. Wang, and W. Qi, "Research progress on nano engineering fluids," *Nanotechnology and Precision Engineering*, vol. 13, no. 3, pp. 167–178, 2015.

[17] O. A. Alawi, N. A. C. Sidik, and A. S. Kherbeet, "Nanorefrigerant effects in heat transfer performance and energy consumption reduction: a review," *International Communications in Heat and Mass Transfer*, vol. 69, pp. 76–83, 2015.

[18] Q. Li and W. Zheng, "Development of study on nanorefrigerant," *Materials Reports*, vol. 30, no. S1, pp. 95–99, 2016.

[19] G. Yu, D. Gao, J. Chen et al., "Experimental research on heat transfer characteristics of CuO nanofluid in adiabatic condition," *Journal of Nanomaterials*, vol. 2016, Article ID 3693249, 7 pages, 2016.

[20] N. Ali, J. A. Teixeira, and A. Addali, "A review on nanofluids: fabrication, stability, and thermophysical properties," *Journal of Nanomaterials*, vol. 2018, Article ID 6978130, 33 pages, 2018.

[21] B. Sahin, E. Manay, and E. F. Akyurek, "An experimental study on heat transfer and pressure drop of CuO–water nanofluid," *Journal of Nanomaterials*, vol. 2015, Article ID 790839, 10 pages, 2016.

[22] S. K. Das, S. U. S. Choi, and H. E. Patel, "Heat transfer in nanofluids—a review," *Heat Transfer Engineering*, vol. 27, no. 10, pp. 3–19, 2006.

[23] D. Guerrieri, F. Viana, S. C. Fragoso, and M. R. Avelino, "Shell-and-tube heat exchangers using nanofluids," in *14 th Bazilian Congress of thermal Science and Engineering*, 2012.

[24] M. Daneshipour and R. Rafee, "Nanofluids as the circuit fluids of the geothermal borehole heat exchangers," *International Communications in Heat and Mass Transfer*, vol. 81, pp. 34–41, 2017.

[25] R. Lotfi, A. M. Rashidi, and A. Amrollahi, "Experimental study on the heat transfer enhancement of MWNT–water nanofluid in a shell and tube heat exchanger," *International Communications in Heat and Mass Transfer*, vol. 39, no. 1, pp. 108–111, 2012.

[26] L. Godson, K. Deepak, C. Enoch, B. Jefferson, and B. Raja, "Heat transfer characteristics of silver/water nanofluids in a shell and tube heat exchanger," *Archives of Civil and Mechanical Engineering*, vol. 14, no. 3, pp. 489–496, 2014.

[27] A. Ghozatloo, A. Rashidi, and M. Shariaty-Niassar, "Convective heat transfer enhancement of graphene nanofluids in shell and tube heat exchanger," *Experimental Thermal and Fluid Science*, vol. 53, pp. 136–141, 2014.

[28] B. A. Bhanvase, S. D. Sayankar, A. Kapre, P. J. Fule, and S. H. Sonawane, "Experimental investigation on intensified convective heat transfer coefficient of water based PANI nanofluid in vertical helical coiled heat exchanger," *Applied Thermal Engineering*, vol. 128, pp. 134–140, 2018.

[29] M. Khoshvaght-Aliabadi, S. Pazdar, and O. Sartipzadeh, "Experimental investigation of water based nanofluid containing copper nanoparticles across helical microtubes," *International Communications in Heat and Mass Transfer*, vol. 70, pp. 84–92, 2016.

[30] P. Sharma, R. Gupta, and R. K. Wanchoo, "Hydrodynamic studies on glycol based Al_2O_3 nanofluid flowing through straight tubes and coils," *Experimental Thermal and Fluid Science*, vol. 82, pp. 19–31, 2017.

[31] A. M. Ardekani, V. Kalantar, and M. M. Heyhat, "Experimental study on heat transfer enhancement of nanofluid flow through helical tubes," *Advanced Powder Technology*, vol. 30, no. 9, pp. 1815–1822, 2019.

[32] S. Pathak, K. Jain, P. Kumar, X. Wang, and R. P. Pant, "Improved thermal performance of annular fin-shell tube storage system using magnetic fluid," *Applied Energy*, vol. 239, pp. 1524–1535, 2019.

[33] P.-Y. Wang, X.-J. Chen, Z.-H. Liu, and Y.-P. Liu, "Application of nanofluid in an inclined mesh wicked heat pipes," *Thermochimica Acta*, vol. 539, pp. 100–108, 2012.

[34] S. Algarni, V. Tirth, T. Alqahtani, P. R. Kshirsagar, and W. Abera, "An empirical analysis of heat expulsion and pressure drop attribute in helical coil tube using nanomaterials," *Journal of Nanomaterials*, vol. 2022, Article ID 9712065, 8 pages, 2022.

[35] D. Jiang, *Research on Heat Transfer of Different Nanofluids in Sandbox Buried Tubes*, Chongqing University, 2020.

[36] G. Diglio, C. Roselli, M. Sasso, and U. Jawali Channabasappa, "Borehole heat exchanger with nanofluids as heat carrier," *Geothermics*, vol. 72, pp. 112–123, 2018.

[37] C. Li, Y. Guan, H. Gao, C. Jiang, J. Li, and R. Yang, "Study on influence of nanofluids on heat transfer characteristics of deep-buried U-bend pipes," *Acta Energiae Solaris Sinica*, vol. 42, no. 1, pp. 392–399, 2021.

[38] H. Hassan and S. Harmand, "Effect of using nanofluids on the performance of rotating heat pipe," *Applied Mathematical Modelling*, vol. 39, no. 15, pp. 4445–4462, 2015.

[39] Y.-F. Niu, W.-L. Zhao, and Y.-Y. Gong, "Experimental investigation of thermal performance of miniature heat pipe using SiO_2–water nanofluids," *Journal of Nanoscience and Nanotechnology*, vol. 15, no. 4, pp. 2932–2938, 2015.

[40] B. S. Bhullar, D. Gangacharyulu, and S. K. Das, "Augmented thermal performance of straight heat pipe employing annular screen mesh wick and surfactant free stable aqueous nanofluids," *Heat Transfer Engineering*, vol. 38, no. 2, pp. 217–226, 2017.

[41] H. Barua, M. Sinaki, and S. Farhad, "Study on geothermal heat exchangers with nanofluids containing ceramic nanoparticles," *Journal of Thermal Science and Engineering Applications*, vol. 15, no. 1, Article ID 011008, 2023.

[42] G. Kumaresan, S. Venkatachalapathy, and L. G. Asirvatham, "Experimental investigation on enhancement in thermal characteristics of sintered wick heat pipe using CuO nanofluids," *International Journal of Heat and Mass Transfer*, vol. 72, pp. 507–516, 2014.

[43] Y. Xuan, Q. Li, X. Zhang, and M. Fujii, "Stochastic thermal transport of nanoparticle suspensions," *Journal of Applied Physics*, vol. 100, no. 4, Article ID 043507, 2006.

[44] Q. Li, *Investigation on Enhanced Heat Transfer of Nanofluids*, NanJing University of Science & Technology, 2004.

[45] Y. Xuan and Q. Li, "Heat transfer Enhancement by nanofluids," *Journal of Engineering Thermophysics*, vol. 04, pp. 466–470, 2000.

[46] K. Wusiman, H. Jeong, K. Tulugan, H. Afrianto, and H. Chung, "Thermal performance of multi-walled carbon nanotubes (MWCNTs) in aqueous suspensions with surfactants SDBS and SDS," *International Communications in Heat and Mass Transfer*, vol. 41, pp. 28–33, 2013.

[47] G. Sriharan, S. Harikrishnan, and H. M. Ali, "Enhanced heat transfer characteristics of the mini hexagonal tube heat sink using hybrid nanofluids," *Nanotechnology*, vol. 33, no. 47, Article ID 475403, 2022.

[48] D. Liu, X. Zhang, F. Tian, X. Liu, J. Yuan, and B. Huang, "Review on nanoparticle-surfactant nanofluids: formula fabrication and applications in enhanced oil recovery," *Journal of Dispersion Science and Technology*, vol. 43, no. 5, pp. 745–759, 2022.

[49] S. Rashidi, L. C. Abdullah, R. Walverkar, M. Khalid, A. Fakhrul-Razi, and M. Y. Faizah, "Stability enhancement of MWCNT/water nanofluids using PVA surfactant," *International Journal of Nanotechnology*, vol. 11, no. 12, pp. 631–639, 2020.

[50] L. Braginsky and V. Shklover, "Thermal conductivity of low-particle-concentration suspensions: correlation function approach," *Physical Review B*, vol. 78, no. 22, Article ID 224205, 2008.

[51] J. Liu, *The Synthesis of Cu Nanoparticles and Their Low Temperature Joining Behavior during Sintering*, Harbin Institute of Technology, 2017.

[52] X. Li, Z. W. Wang, and Y. F. Sun, "Research of surfactant on the influence of nanofluid," *Materials Reports*, vol. 29, no. 23, pp. 30–35, 2015.

[53] Q. Li, Y. Xuan, J. Jiang, and J. W. Xu, "Experimental investigation on flow and convective heat transfer feature of a nanofluid for aerospace thermal management," *Journal of Astronautics*, vol. 04, pp. 391–394 414, 2005.

[54] Q. Li and Y. Xuan, "Copper–water nanofluid flow and convective heat transfer characteristics," *Scientia Sinica (Technologica)*, vol. 03, pp. 331–337, 2002.

[55] JGJ, "Specification for mix proportion design of ordinary concrete," 2011.

[56] X. Ou, *Research on High Efficient Cooling Technology of Injection Mold Based on Nanofluid*, South China University of Technology, 2016.

[57] B. Zhang, *Research on Heat Transfer Performance of Ground Heat Exchanger for Ground Source Heat Pump*, Hebei University of Technology, 2022.

[58] K. Y. Leong, R. Saidur, and T. M. I. Mahlia, "Modeling of shell and tube heat recovery exchanger operated with nanofluid based coolants," *International Journal of Heat and Mass Transfer*, vol. 55, no. 4, pp. 808–816, 2012.